https://doi.org/10.7494/miag.2021.1.545.7

ANDRZEJ FRĄCZEK

Engineering project of a mobile robot with a metal detector for landmine detection

This paper presents the design of a mobile tracked robot capable of moving in varied terrain. Its task is to detect metal objects, which is achieved by means of a metal detector placed on a manipulator with three degrees of freedom. The whole system is controlled from a phone using a dedicated application. For the mechanical parts, a mathematical model was created, which was used to carry out driver selection and other essential components. For the detector, a description of research carried out to select the coil of the sensory system is presented. In the part related to the control of the robot, the application and the process of testing by means of a station made on a prototype board is presented. Finally, the assembly of the entire robot is presented along with conclusions and directions for further research.

Key words: *mobile robot, manipulator, metal detector, Bluetooth app*

1. INTRODUCTION

In the 20th century, a number of conflicts took place in Europe and the Middle East: with among the most notable being World War I and II, the war in Afghanistan, and the conflict in the former Yugoslavia. This led to an increase in the use of mines, guns, aircraft and many other military items.

Ones of the most unpredictable threats are mines. According to Hemapala [1], up to 100,000,000 anti-personnel mines have been deployed worldwide by various military units and terrorist organisations. Cheap to produce, invisible to the enemy, they can cause horrific damage.

Unfortunately, when the warring parties exit the area of operations, usually at the end of a conflict, they leave behind many dangerous explosives which pose a threat to the civilian population. The process of clearing such areas is extremely time-consuming. It requires the use of qualified personnel with modern equipment and the clearing operation itself is a life and health-threatening activity for the operator. In Poland alone, naval units carry out 300 interventions a year in the coastal zone to neutralise mines and explosives that could pose a threat to civilians [2].

Simultaneously many have recognised the possibility of using remotely controlled machines to neutralise a variety of explosives. Robots provide a safer and more secure solution for the operator. Such constructions are now the basis for sappers in modern armed conflicts.

Many of these designs were developed in collaboration with the military segment. They can be divided into two types. The first is an infantry support vehicle (a perfect example is MATILDA robot used by American soldiers during the Iraqi conflict [3]). The second category are robot prototypes designed to operate in harsh environments such as water. A description of these structures (ARIEL or BUR-001) was presented in Jankiewicz [4].

At the same time, prototypes of structures designed to clear the area and allow civilians to return are being built in universities around the world. These include the DYLEMA walking-robot with hexapod configuration [5], a five degrees of freedom manipulator mounted on a remote controlled commercially available 4-wheeled ATV GRYPHON [6] or solar-powered mobile metal detector robot [7].

However, such structures are extremely expensive to manufacture and operate. The problem of unexploded ordnance/mines unfortunately affects the whole globe (often in countries just recovering from conflicts and which cannot afford expensive equipment). Engineers from such countries (e.g. Pakistan) are trying to find a remedy, a result of which is the MARWA robot [8].

These were aspects that motivated the design of a low-cost robot that could help identify and clear dangerous areas. Such a solution would be more achievable for poorer countries and could prevent unnecessary injuries.

2. MECHANICAL PART

The objectives for the mobile platform were as follows:

- the ability of the robot to move in both terrain (grass, sand) and urban parts (paving stones, asphalt),
- ease in overcoming uneven terrain,
- the lowest possible impact on the ground structure (to prevent deformation of the terrain).

Based on an analysis of the classic solutions available on the market, a tracked system was chosen (Fig. 1).

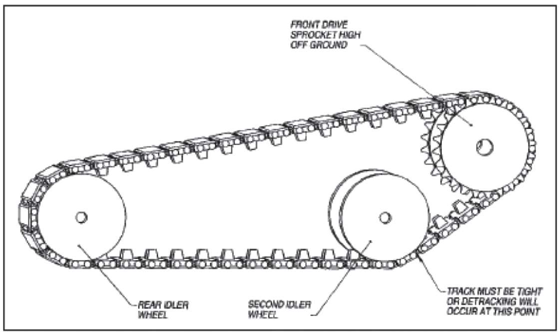

Fig. 1. Tracked vehicle drivetrain [9]

The biggest advantage of this type of locomotion (over wheeled suspension) is the possibility of operating in difficult terrain (mud, snow). The meshing length is considerably longer than that of the wheel tyres of a wheeled vehicle, so that only on extremely soft ground cans the track slip in relation to the ground [10].

In addition, thanks to the continuous tracks, the surface pressure is at a lower level. A modern M1A2 Abrams tank with a weight of nearly 72 tons equipped with such a system has a similar pressure as a man standing on one leg (82 kPa) [9].

In addition, a discussion was held regarding the type of suspension of the robot. The robot is expected to operate on undulating terrain full of rocks and vibrations may have an adverse effect. Due to the nature of the robot's work (low speed of movement is preferred in order to increase the accuracy of the search) a solution with rigid wheels will be used.

According to Sandin [9], the phenomenon of vibration at low speeds disappears, so this variant can easily be used in this project.

The next move was to formulate the mathematical model, and this needed to be divided into two segments:

- kinematics and dynamics of the continuous tracks,
- mechanics of the tracked vehicle.

Each of these has a different but significant impact on the movement of the entire mobile platform.

Upon first consideration, we can think of the caterpillar track as a flexible, inextensible belt. It constitutes a circumference defined by a non-deformable substrate, a driving and tensioning wheel and support wheels. Each point of the caterpillar circumference participates in two movements:

- relative to the road on which the vehicle is moving,
- relative to the vehicle.

The first factor affecting the platform is skidding. It occurs when the vehicle speed differs from the relative speed. This quantity is described by the slip coefficient:

$$s = 1 - \frac{v}{v_R} \tag{1}$$

where:

v – vehicle speed [m/s],
v_R – speed of the point on the perimeter of the track [m/s].

For the purposes of the following considerations, the caterpillar model was changed into separate components that affect its motion. Using the considerations carried out in Burdzinski [11], the concept of average speed is introduced. This is due to the fact that the angular velocity of the driving wheel is variable. This is influenced by the fact that the tracked vehicle is a dynamic system operating on non-uniform ground. In addition, the finite pitch length of the track is an influence. The formula for the average speed v_{sr} [m/s] is as follows:

$$v_{sr} = t_g n_k z(1 - s) \tag{2}$$

where:

t_g – track scale [m],
z – number of drive wheel teeth,
n_k – number of revolutions of the drive wheel [rad/s].

The last thing to consider is the efficiency of the track. Friction losses occur during the relative movement of two adjacent links. These depend on the track tension, centrifugal forces and driving torque. The formula itself is very complicated and in Burdzinski [11] an alternative, formula of efficiency coefficient is used to simplify calculations:

$$\eta_g = 0.95 - 0.005 v_{sr} \tag{3}$$

The next move was to form a model for the whole platform.

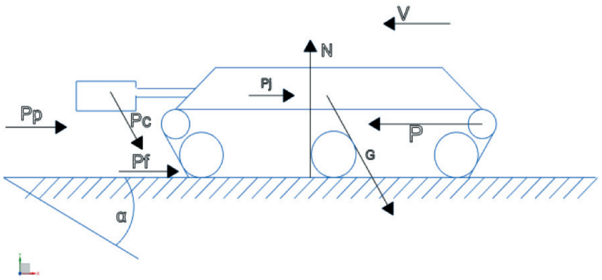

Fig. 2. Forces acting on the vehicle

Figure 2 shows the forces acting on a vehicle moving up a hill with an angle to the vertical of α. These are:

P – driving force [N],
N – ground reaction force [N],
P_p – aerodynamic drag force [N],
P_f – rolling resistance [N],
P_c – weight of the coil [N],
G – weight of the robot [N],
P_j – inertia force [N].

The following forces will be discussed below:

1) Gravity force of the robot – is applied at the centre of gravity. It includes the masses of both the body itself and the manipulator with coil.
2) Rolling resistance – for tracked vehicles the description of this force is complex, therefore according to Burdzinski [11] this force can be described by the equation:

$$P_f = f(G + P_C)\cos\alpha \tag{4}$$

where f – rolling resistance coefficient.

3) Ground reaction force – in the robot is the resultant force of the ground action on the lower crawler belt. The value can be determined from the equation:

$$N = (G + P_C)\cos\alpha \tag{5}$$

4) Aerodynamic drag force – this is a result of air acting on the geometry of the vehicle and can be expressed by the formula:

$$P_p = \rho c A v^2 \tag{6}$$

where:

ρ – air density [kg/m^3],
c – aerodynamic drag coefficient,
A – reference area [m^2].

5) Inertia force – occurs for a non-inertial reference system and is applied at the centre of gravity of the vehicle, and its formula is:

$$P_J = (G + P_C)\frac{dv}{dt} \tag{7}$$

6) Driving force – arises as a result of the drive system. For unsteady motion, this formula has the equation:

$$P = \frac{M_k}{r_k}\eta_g - \frac{M_j}{r_k} \tag{8}$$

where:

M_k – torque from the drive wheel [Nm],
r_k – drive wheel radius [m],
M_j – the tangential moment of inertia of all rotating parts of the track with respect to the drive wheel axis [Nm].

Finally, after ordering and introducing assumptions, the formulas can be obtained:

1) For uniform rectilinear motion, the members containing dv/dt. In addition, for assumed speeds of motion, the effect of air resistance can be neglected and the equation is of the form:

$$\frac{M_k}{r_k}\eta_g = f(G + P_C)\cos\alpha + (G + P_C)\sin\alpha \tag{9}$$

2) For moving on flat terrain, the angle α equals 0, so:

$$\frac{M_k}{r_k}\eta_g = f(G + P_C)\cos\alpha \tag{10}$$

Once the equations are derived, calculations will be made for the minimum torque that needs to be delivered to the drivetrain. The assumptions are to move at a speed of 0.4 m/s on a gradient of 10 degrees (for normal roads this corresponds to a percentage gradient of 17.63%. For comparison, the highest hills in the Alps are 32% [11]).

In addition, it is still necessary to assume a safety factor. In the literature it is 1.15 for a vehicle with a constant load [11]. However, since this is a pioneering design, the safety factor $n = 1.4$ was adopted. The final moment obtained is:

$$M_k = 0.56\ \mathrm{Nm} \tag{11}$$

For this moment, the following were selected:

- caterpillar tracks system,
- Pololu brand DC motors,
- dedicated controllers for the motors,
- fans to cool the systems.

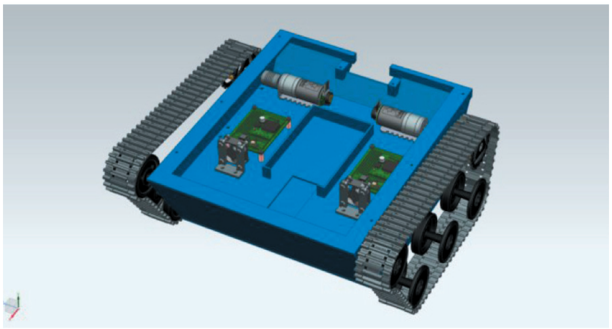

Fig. 3. CAD model of the mobile platform

To verify that all the components will fit correctly in the robot body, a suspension model was made with the components already selected, which is shown in Figure 3. The body is prepared to be fabricated using 3D printing technology.

The next step was the construction of the manipulator. The following requirements were set:

- possibility of carrying out measurements at a precisely defined height above the ground,
- "sweeping" operations (sensing a larger area for a single robot position).

A manipulator with the first three degrees of freedom (DOF) will be used in this project because these are sufficient to meet the above design objectives. This is because they are concerned with moving the coil in space and not positioning it relative to the ground.

After completing the analysis of the most common kinematic structures, the RRR (rotating anthropomorphic manipulator arm) structure will be used because it is characterised:

- universal application,
- large working area,
- reliability.

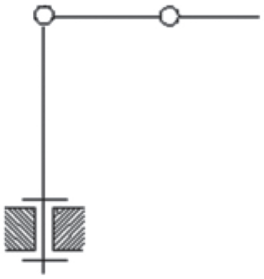

Fig. 4. Rotating anthropomorphic manipulator arm [12]

It also has disadvantages such as the high cost of a highly repeatable manipulator, but for ground search operations this is unnecessary and would generate additional costs.

In the next phase the Denavit–Hartenberg notation was used to obtain the uniform transformation matrix:

$$T_3^0 = \begin{bmatrix} c_1 c_{23} & -c_1 s_{23} & s_1 & c_1\left(a_2 c_2 + a_3 c_{23}\right) \\ s_1 c_{23} & -s_1 s_{23} & c_1 & s_1\left(a_2 c_2 + a_3 c_{23}\right) \\ s_{23} & c_{23} & 0 & a_2 s_2 + a_3 s_{23} \\ 0 & 0 & 0 & 1 \end{bmatrix} \tag{12}$$

Based on this and the complex points to be reached by the manipulator, the lengths of the manipulator members were selected. For this, the method developed in the work of Siciliano, Sciavicco, Villani and Oriolo was used [13].

The next step was the selection of drives. A mathematical model was formulated for each member separately and the torque required to move that member and servo was calculated based on that model (Fig. 5).

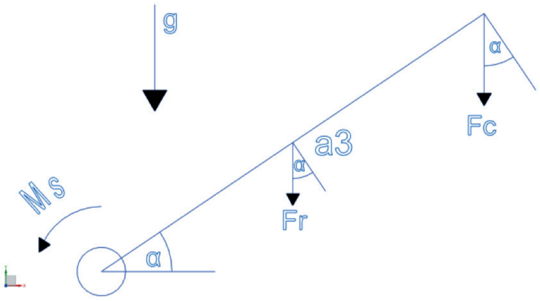

Fig. 5. Forces acting on third arm

In the last part, the goal was to make a CAD model of the individual components and the assembly with the servos. The finite element method analysis was performed for the manipulator thus prepared. The assembly of the whole element is presented in Figure 6.

Fig. 6. CAD model of the manipulator

The material from which the manipulator components will be made is ABS plastic. The use of plastic which can be used as a filament in the 3D printer of FDM type has a number of advantages:

- when using metal as a construction material, the measuring system which is supposed to detect metal in the environment is disturbed – this is a key feature,
- ABS plastic used in printers is characterized by high strength and resistance to weather conditions.

3. ELECTRONIC PART

The system that is mainly used when searching for metal in the ground is a metal detector. This system operates using Faraday's law and the generalized Ampere's law.

According to Halliday, Walker and Resnick [14], Faraday's law is formulated as follows: "An electric field is induced by the time-varying flux of a magnetic field".

$$E = -\frac{d\Phi_B}{dt} \tag{13}$$

where:

$\frac{d\Phi_B}{dt}$ – rate of change in magnetic flux [Wb/s],

E – electromotive force [V].

According to Halliday, Walker and Resnick [14], Ampere's generalized law is formulated as follows: "The source of a magnetic field is an electric current or a time-varying electric field flux".

$$\int \vec{B}\overrightarrow{dl} = \mu_0 \varepsilon_0 \frac{d\Phi_E}{dt} + \mu_0 I \tag{14}$$

where:

$\int \vec{B}\overrightarrow{dl}$ – the closed line integral of the magnetic field around a closed curve [T],

μ_0 – vacuum permeability [H/m],

ε_0 – vacuum permittivity [F/m],

$\frac{d\Phi_E}{dt}$ – rate of change in electric flux [Vm],

I – electric current [A].

The detector generates a magnetic field by means of an electrical circuit. The sensor starts to fulfil its task when it is in an area where electromagnetic waves start to interact with conductive material, e.g. in the ground. An electromotive force is then induced in the object (Faraday's law). So-called eddy currents begin to form, which are the cause of the induced magnetic field (generalised Ampere's law). The new magnetic field starts to act on the coil. Current starts to flow and is registered by the detector's measuring system.

The properties of the second field depend on many parameters. These include the geometry of the object itself (distance from the detector, orientation towards it), material properties (shape, size, conductivity, magnetic permeability). The size and shape of the coil itself are also very important as shown in Figure 7.

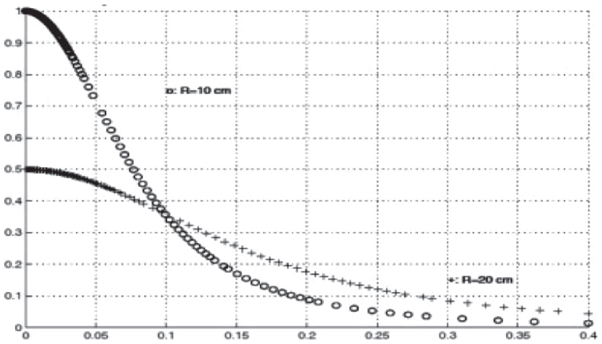

Fig. 7. Dependence of the magnetic field for two different coil sizes [15]

The normalized graph above shows the dependence of the magnetic field on the distance d [m] from them for two different coil sizes (10 cm and 20 cm). The normalisation was carried out for the smaller coil at a distance $d = 0$ [15].

There are several types of metal detectors on the market. After the analysis of metal detector types, the PI (Pulse Induction) type was selected.

These sensors work by regularly generating electrical pulses sent to the probe. When the electrical pulse disappears, the magnetic field on the probe disappears. The time it takes for the field to disappear depends on whether there is a metal present. If there is, the field fades much more slowly which can be detected. Its advantages are:

- no sensitivity to soil mineralisation,
- simple design (only one probe needed).

Making a metal detector yourself is difficult. The number of variables affecting the operation is large, so the cost of ready-made detectors starts at 300 zloty (65 euro). In addition, one of the objectives was to take measurements, making different coils in order to find the optimal value of parameters such as diameter and number of coils. The kit called J-297 for self-assembly by Jabel company was used.

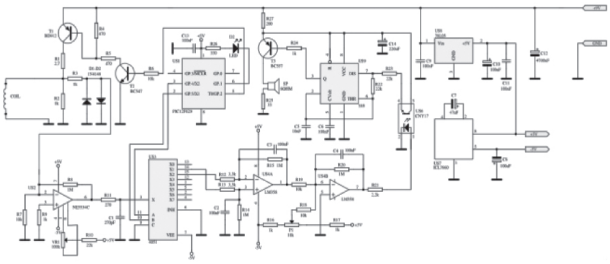

Fig. 8. Metal detector board Jabel J-297

As mentioned earlier, a lot depends on the parameters of the detector coil and thus for this purpose it was planned to carry out measurements. The purpose of the analysis was to optimize the coil dimensions (which depend on two parameters):

- number of coil windings,
- coil diameter.

The goal was to keep the weight as low as possible while obtaining the best metal detection results.

Due to the selected target dimensions of the robot, two coil diameters were chosen to be used for optimization: 10 cm and 12 cm. A suitable “pad” (a 3D printout consisting of a base and a number of vertical columns used to facilitate the coil winding process) on which coils was made with the parameters shown in Table 1.

Table 1
Prepared coils

Coil number	Coil diameter [cm]	Number of turns	Weight [g]
1	10	50	46.9
2	10	70	65.6
3	10	95	89.0
4	12	40	45.0
5	12	60	67.5

Two measurement sites were selected:

- Bulgarian lev 1 coin (diameter 24.5 mm, thickness 1.9 mm),
- metal can 0.33 l of a well-known cola beverage producer (height 116 mm, width 66 mm, depth 66 mm).

A measurement rig was made for the measurements (Fig. 9). The object is placed on a printed platform which is moved up and down by a string which forms a straight line by means of a block. When the detector detects a coin, the string can be restrained by weaving it several times through the printed piece located on the bottom shelf of the table. This eliminates the error caused by hand trembling.

Fig. 9. Measuring stand for a coin

The following brief plan was adopted for making measurements:

1) turning on the detector,
2) calibrating the locator,
3) take 5 measurements,
4) turn off the locator.

For each object this procedure was repeated 3 times. The measurement results are shown in the following Table 2 and the symbol descriptions are:

- mean value: μ [cm],
- standard deviation: σ [cm].

Using all the measurements taken, a 12 cm 60 turns coil was finally selected.

The way the operator communicates with the robot is also an important issue. Design assumptions:

- simplicity of operation,
- lack of autonomy of the robot (the user controls the movement of the robot).

Table 2

Summary of measurement results

Coil	µ can [cm]	σ can [cm]	µ coin [cm]	σ coin [cm]
1	25.91	2.29	11.33	0.15
2	25.69	0.93	12.14	0.3
3	26.52	2.9	13.66	0.5854
4	26.13	1.64	14.12	0.42
5	29.73	1.19	60.0	0.27

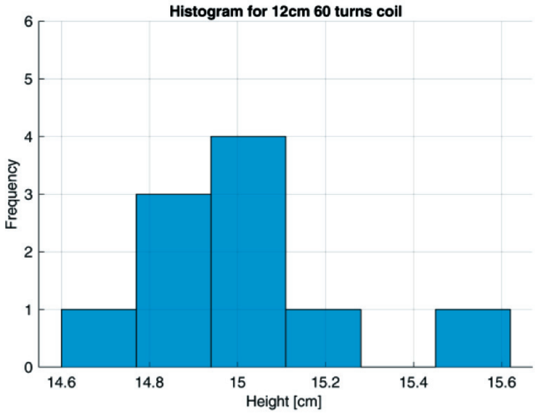

Fig. 10. Example histogram from measurements

The Bluetooth standard was chosen. BLE (Bluetooth Low Energy) ensures very low energy consumption and a range of up to 20 m.

In addition, it is possible to create a dedicated application for Android phones, which can be developed on an on-going basis.

The application was written on appinventor.mit.edu. This website allows you to write Android applications without using conventional programming languages. In this environment, applications are executed using blocks corresponding to specific actions (e.g. sending a single-bit signal using Bluetooth).

After creating all the necessary functions, the application was compiled and saved as a file with the extension .app. This file is supported by most of the currently popular phone brands. The appearance of the application after installation on the phone is shown in Figure 11.

The code created for the operation of the microcontroller itself was written in Arduino IDE environment. The library “Servo” was used. The design of the program itself is based on *switch...case* commands to ensure the readability and clarity of the code. For the purposes of testing the Android application, a test bench was made using a prototype board and manipulator (Fig. 12).

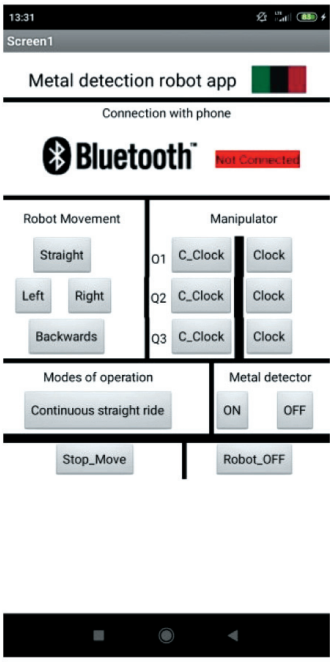

Fig. 11. Screenshot of the application from a private phone

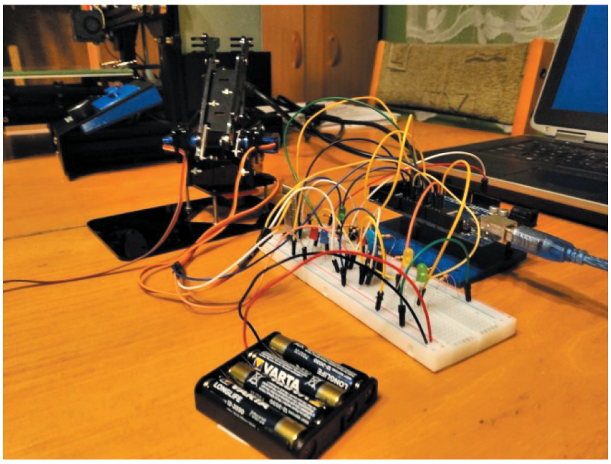

Fig. 12. Mobile application test bench

The signalling of individual functions for the mobile platform and the detector was realised by means of LEDs. This allows for a cheap and easy way to test the communication of these functions.

At the end, a control board was selected. The Arduino Mega microcontroller will be used to control the whole system (Fig. 13).

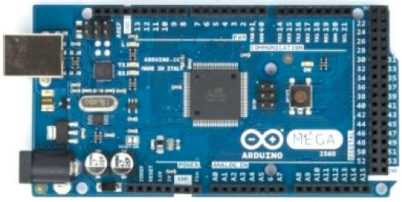

Fig. 13. Arduino Mega

It is widely available on the market, offering an affordable price and a large number of ports for connecting peripheral elements which is shown in Figure 13.

4. ROBOT ASSEMBLY

With the work completed and all the important electrical components selected, the final step was to select the power supply and inverters that would ensure that adequate voltage was continuously supplied to the motors and servos. The Li-Pol cell was chosen because it is commonly used in robotics. The converters, on the other hand, were selected from the Pololu company catalogue.

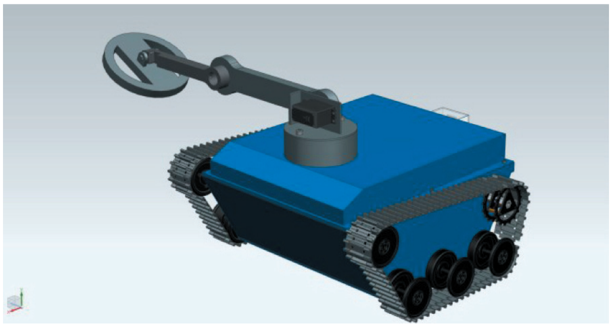

Fig. 14. CAD model of the robot – front side view

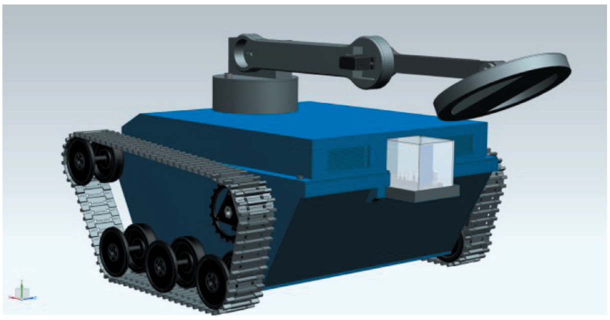

Fig. 15. CAD model of the robot – rear side view

After selecting all the components, the whole robot was assembled and is depicted in Figures 14 and 15. The whole robot weighs about 3.5 kg.

5. SUMMARY

The goal that was set before the work started, i.e. the design of the robot, has been achieved. Thanks to such an extensive scope of work, it was possible to apply the knowledge acquired during the first degree studies. Detailed issues included mechanics, drive selection, manipulator kinematics, metal detector testing and programming.

At the same time, this is a project. Its full verification will only be possible when the robot itself is built. Exploitation and tests of the prototype may generate situations that cannot be foreseen at the stage of creation of assumptions and design. However, this does not mean that the design phase can be neglected. During this phase, costly mistakes can be avoided which would otherwise only be discovered at further stages of the project and would result in the need to change the construction and entail additional costs.

In addition, after becoming familiar with solutions present on the market, it is worth considering whether it would be a good idea to enrich the robot design with additional functions. In most designs there is a gripper at the end of the manipulator, which allows positioning the sensory system in relation to the curvature of the ground.

Another important thing would be to test the detector for objects in the soil. The Jabel system has met its objectives for tests in the air, but its performance can significantly deteriorate when searching in the ground, so it is worth checking its performance in this area. Additionally, in the electronics part, the addition of ultrasonic cameras/sensors could be considered to increase the autonomy of the robot.

In the software part, the tests carried out on the prototyping board allowed us to stabilise the communication with the Bluetooth module, but it was impossible to reproduce in 100% the functioning of the robot. One of the most important things is the encoder, which is placed in the motors responsible for controlling the mobile platform. It is an extremely valuable element as it allows precisely controlling the robot and improving the smoothness of the system itself (a regulator can be used). It was not possible to test this on the prototype board, so until possible tests on the robot prototype it is necessary to include encoders in the robot control algorithm.

6. CONCLUSIONS

The intended outcome of the exploration robot design has been achieved. In future work, its further development and practical implementation is needed to obtain fully functional metal detector robot.

References

[1] Hempala U.M.: *Robots for Humanitarian Demining*. InTech, 2017.

[2] Chmieliński M.: *Bezpieczeństwo neutralizacji niewypałów i niewybuchów amunicji artyleryjskiej w strefie przybrzeżnej.* Autobusy 2017, 6: 99–106.

[3] Munkeby S., Jones D., Bugg G., Smith K.: *Applications for the MATLIDA Robotic Platform*. Proceedings SPIE 2002, 4715, 206–2013.

[4] Jankiewicz M.: *Przeciwminowe roboty – pojazdy kroczące*. Biuletyn WAT 2017, 56: 273–286.

[5] Gonzalez de Santos P., Garcia E., Estemera J., Armada M.A.: *DYLEMA: Using walking robots for landmine detection and location*. International Journal of Systems Science 2005: 545–558.

[6] Fukushima F. E., Freese M., Matsuzawa T., Aibara T., Hirose S.: *Humanitarian demining robot Gryphon current status and an objective evaluation*. International Journal on Smart Sensing and Intelligent Systems 2017: 735–753.

[7] Albert F.Y.C., Mason C.H.S., Kiing C. K. J., Ee K.S., Chan K.W.: *Remotely operated solar-powered mobile metal detector robot*. Procedia Computer Science 2014, 42: 232–239.

[8] Abubakr M., Syed M.A., Talha M., Adnan M., Syed A.A., Mhequb H., Ali A., Mian A.M.: *Marwa: A Rough Terrain Landmine Detection Robot For Low Budget*. Proceedings of the 43rd International Symposium on Robotics, London 2012.

[9] Sandin P.: *Robot Mechanisms and Mechanical Devices Illustrated*. McGraw Hill, New York 2003.

[10] Rybak P.: *Tracked or wheeled chassis*. Journal of KONES Powertrain and Transport 2007, 3: 527–536.

[11] Burdziński Z.: *Teoria ruchu pojazdu gąsienicowego*. Wydawnictwo Komunikacji i Łączności, Warszawa 1972.

[12] Buratowski T.: *Teoria robotyki*. Wydawnictwo AGH, Kraków 2012.

[13] Siciliano B., Sciavicco L., Villani L., Oriolo.: *Robotics Modelling, Planning and Control*. Springer, London 2010.

[14] Halliday D., Walker J., Resnick R.: *Podstawy fizyki. Tom 3*. Wydawnictwo Naukowe PWN, Warszawa 2015.

[15] Bruschini C.: *A multidisciplinary analysis of frequency domain metal detectors for humanitarian demining*. Ph.D. thesis, Vrije Universiteit Brussel, Brussels 2002.

ANDRZEJ FRĄCZEK, Eng.
AGH University of Science and Technology
al. A. Mickiewicza 30, 30-059 Krakow, Poland
anfracze@student.agh.edu.pl